
Research Article: New Research | Development

Increased RET activity coupled with a reduction in the *RET* gene dosage causes intestinal aganglionosis in mice

<https://doi.org/10.1523/ENEURO.0534-20.2021>

Cite as: eNeuro 2021; 10.1523/ENEURO.0534-20.2021

Received: 8 December 2020

Revised: 24 March 2021

Accepted: 13 April 2021

This Early Release article has been peer-reviewed and accepted, but has not been through the composition and copyediting processes. The final version may differ slightly in style or formatting and will contain links to any extended data.

Alerts: Sign up at www.eneuro.org/alerts to receive customized email alerts when the fully formatted version of this article is published.

Copyright © 2021 Okamoto et al.

This is an open-access article distributed under the terms of the Creative Commons Attribution 4.0 International license, which permits unrestricted use, distribution and reproduction in any medium provided that the original work is properly attributed.

1 **Manuscript title:**

2 **Increased RET activity coupled with a reduction in the *RET* gene dosage causes**
3 **intestinal aganglionosis in mice**

4

5 Abbreviated Title: RET-activating mutation causing ENS deficits

6

7 Authors: Mitsumasa Okamoto, Toshihiro Uesaka, Keisuke Ito and Hideki Enomoto

8

9 Affiliation: Division for Neural Differentiation and Regeneration, Department of
10 Physiology and Cell Biology, Kobe University Graduate School of Medicine, Kobe,
11 Hyogo, Japan

12

13 Author Contributions: TU and HE Designed Research; MO, TU and KI Performed

14 Research: HE wrote the paper

15

16 Correspondence should be addressed to Hideki Enomoto at
17 enomotoh@med.kobe-u.ac.jp

18

19 Number of Figures 5

20 Number of Tables 0

21 Number of Multimedia 0

22 Number of words of Abstract 178

23 Number of words for Significance of Statement: 115

24 Number of words for Introduction: 620

25 Number of words for Discussion: 810

26

27 **Acknowledgements**

28 The authors thank Hazuki Hiraga for editing this manuscript.

29

30 **Conflict of Interest**

31 The authors report no conflict of interest.

32

33 **Funding sources**

34 This work was supported by Japan Society for the Promotion of Science, Japan, Grant

35 17H03550, 17K19527, 16K08466, Grants-in-Aid for Scientific Research on Innovative

36 Areas “Stem Cell Aging and Disease” (#25115002) from MEXT, Takeda Science
37 Foundation, and Yakult Bio-Science Foundation.

38 **Abstract**

39 Mutations of the gene encoding the *RET* tyrosine kinase causes Hirschsprung disease
40 (HSCR) and medullary thyroid carcinoma (MTC). Current consensus holds that HSCR
41 and MTC are induced by inactivating and activating *RET* mutations, respectively.
42 However, it remains unknown whether activating mutations in the *RET* gene have
43 adverse effects on ENS development in vivo. We addressed this issue by examining
44 mice engineered to express *RET*^{51(C618F)}, an activating mutation identified in MTC
45 patients. Although *Ret*^{51(C618F)/51(C618F)} mice displayed hyperganglionosis of the ENS,
46 *Ret*^{51(C618F)/-} mice exhibited severe intestinal aganglionosis due to premature neuronal
47 differentiation. Reduced levels of GDNF, a *RET*-activating neurotrophic factor,
48 ameliorated the ENS phenotype of *Ret*^{51(C618F)/-} mice, demonstrating that
49 GDNF-mediated activation of *RET*^{51(C618F)} is responsible for severe aganglionic
50 phenotype. The *RET*^{51(C618F)} allele showed genetic interaction with *Ednrb* gene, one
51 of modifier genes for HSCR. These data reveal that proliferation and differentiation of
52 ENS precursors are exquisitely controlled by both the activation levels and total dose of
53 *RET*. Increased *RET* activity coupled with a decreased gene dosage can cause intestinal

54 aganglionosis, a finding that provides novel insight into HSCR pathogenesis.

55

56

57 **SIGNIFICANCE STATEMENT**

58 Mutations of the *RET* gene have been identified in Hirschsprung disease (HSCR) and
59 neuroendocrine tumors (NET). It has been thought that HSCR and NET are caused by
60 inactivating and activating mutations of the RET gene, respectively. However, little is
61 known about whether enhanced RET activity exerts any roles in the pathogenesis of
62 HSCR. We show that mice carrying an activating mutation in the *Ret* gene display
63 intestinal aganglionosis when the *Ret* gene dosage is halved. The aganglionosis
64 phenotype is caused by premature neuronal differentiation and impaired migration of
65 ENS precursors. These findings raise the possibility that RET-activating mutations can
66 cause HSCR when associated with a reduction in the dosage or expression of the *RET*
67 gene.

68

69

70 **Introduction**

71 RET is a receptor tyrosine kinase that serves as a signaling receptor for the glial
72 cell-derived neurotrophic factor (GDNF) family ligands (GFLs) (Baloh et al., 2000;
73 Airaksinen and Saarna, 2002). Binding of GFLs to their cognate GFR α receptors
74 induces dimerization and subsequent autophosphorylation of RET, culminating in the
75 activation of downstream intracellular signaling. RET is expressed in a wide variety of
76 neural crest (NC)-derived cell types and endoderm-derived thyroid C cells. In humans,
77 mutations in the *RET* gene are associated with the pathogenesis of various forms of
78 diseases that include Hirschsprung's disease (HSCR) and medullary thyroid carcinoma
79 (MTC). Hereditary MTCs occurs in multiple endocrine neoplasia (MEN) 2, which is
80 further subcategorized into MEN2A, MEN2B and familial medullary thyroid carcinoma
81 (FMTC) based on the phenotype such as pheochromocytoma, hyperparathyroidism
82 and/or other developmental anomalies (infertility, marfanoid habitus etc.) (Wells et al.,
83 2013; Tomuschat and Puri, 2015).

84 HSCR is characterized by the congenital loss of enteric ganglia in the distal portion of
85 the gut (intestinal aganglionosis). Genetic studies have revealed that HSCR is a
86 multifactorial disease that involves mutations in multiple genes for its pathogenesis and
87 exhibits complex patterns of inheritance. To date, mutations have been identified in as

88 many as 17 genes (Tilghman et al., 2019), and, among which the RET gene is most
89 frequently mutated (Amiel et al., 2008). HSCR-associated RET mutations have been
90 identified throughout the *RET* genome, affecting both coding and non-coding regions.
91 Coding mutations account for only 50% of familial and 15% of sporadic cases of HSCR
92 (Edery et al., 1994; Romeo et al., 1994). Meanwhile, some non-coding variants that
93 potentially affect the enhancer activity of the RET gene are considered necessary, albeit
94 not sufficient, mutations in isolated HSCR cases (Kapoor et al., 2015). Thus, HSCR is a
95 complex genetic trait in which reduced RET expression confers susceptibility to the
96 disease.

97 In contrast to HSCR, MEN2 displays rather simple genetic features. Most of those
98 mutations affects a restricted cysteine residue in the extracellular domain of RET,
99 converting it to arginine, tyrosine or phenylalanine. These amino acid conversions
100 disrupt intra-molecular cysteine bonding and causes aberrant inter-molecular bonding
101 and successive auto-phosphorylation of RET, leading to its aberrant and
102 ligand-independent activation. Those RET mutations are likely sufficient for the
103 development of tumors because familial MEN2 cases demonstrate autosomal dominant
104 inheritance (Margraf et al., 2009).

105 Together, HSCR- and MTC-associated RET mutations display distinct features, and,

106 although the whole spectrum of biological effects by those RET mutations have not
107 been fully elucidated, current consensus holds that HSCR is caused by inactivating
108 mutations of the *RET* gene whereas MTC is induced by activating mutations of RET
109 (Hansford and Mulligan, 2000).

110 Although previous studies support that inactivation or downregulation of RET signaling
111 leads to HSCR-like intestinal aganglionosis in mice, it has not been clear whether
112 activating mutations of RET have adverse effects on ENS development (Amiel et al.,
113 2008). To address this issue, we examined the development of the ENS in mice
114 engineered to express RET C618F, one of the MTC-associated RET-activating mutants,
115 under the endogenous *Ret* promoter (Okamoto et al., 2019). Biochemical studies
116 revealed that RET C618F displays slightly higher RET basal phosphorylation than
117 normal, but still requires GDNF for its full activation (Okamoto et al., 2019). Thus, RET
118 C618F mutant mice are an ideal platform to understand how the ENS develops when
119 the activity of RET is slightly elevated. We found that, in mice carrying the RET C618F
120 mutation, the ENS phenotype changed dramatically from hyperganglionosis to
121 aganglionosis when the *Ret* gene dosage was changed from two copies to one copy.
122 Premature neuronal differentiation of ENS precursors contributed to the aganglionosis
123 phenotype. Our findings reveal a novel mechanism of HSCR pathogenesis that is

124 Ret-activating mutations can cause HSCR when the Ret gene dosage is reduced.

125

126 **Methods**

127 Mice

128 The generation and characterization of *Ret51* and *Ret51(C618F)* mice have been
129 described previously (Okamoto et al., 2019). We obtained *Ret^{GFP}* (a kind gift from J.
130 Milbrandt, Washington University School of Medicine (Jain et al., 2006), *Gdnf^{+/-}* (a
131 kind gift from V. Pachnis The Francis Crick Institute, London, UK (Moore et al., 1996),
132 and *Ednrb^{flex3}* mice (a kind gift from M.L. Epstein, University of Wisconsin-Madison
133 (Druckenbrod et al., 2008)). *Ednrb^{+/-}* mice were obtained by crossing *Ednrb^{flex3}* mice to
134 *Actb::Cre* mice (Stock No: 019099; Jackson Laboratories (Lewandoski et al., 1997)).

135 Mice were bred and maintained at the Institute of Experimental Animal Research of
136 Kobe University Graduate School of Medicine under specific pathogen-free conditions
137 and all animal experiments were performed according to the Kobe University Animal
138 Experimentation Regulations.

139

140 *Whole-mount immunostaining*

141 Dissected gut from embryos or P0 pups were fixed with 4% paraformaldehyde (PFA) in
142 PBS containing 10mM phosphate buffer, pH7.4, 137mM sodium chloride, and 2.7 mM
143 potassium chloride overnight at 4°C and incubated in 1% Triton X-100 in PBS for 30

144 min at room temperature. After fixation and permeabilization, the preparations were
145 incubated in 0.1 M glycine in PBS for 2-6 hours and processed for
146 immunohistochemistry. For the preparations from P0 pups, blocking solution contains
147 5% skim milk, 5% DMSO, 1% Tween20 in PBS. The following antibodies were used:
148 guinea pig anti-Phox2b (1:1000, home-made, raised against the C-terminal region of
149 Phox2b (RRID:AB_2313690) (Pattyn et al., 1997); goat anti-Sox10 (1:300,
150 Cat.#sc-17342, Santa Cruz Biotechnology Inc., RRID: AB_2195374); rabbit
151 anti-PGP9.5 (1:1000, Cat.#RA-95101, Ultra Clone, RRID: AB_2313685); rabbit
152 anti-phospho-ERK1/2 (1:500, Cat.#9101, Cell signaling Technology, RRID:
153 AB_331646) and chicken anti-GFP (1:1000, Cat.#GFP-1020, Aves Laboratories, RRID:
154 AB_10000240). We used the following secondary antibodies (Biotium): CF488A
155 donkey anti-rabbit IgG (Cat.#20015, RRID: AB_10559669), CF488A donkey
156 anti-chicken IgY (Cat.#20166, RRID: AB_10854387), CF568 donkey anti-guinea-pig
157 IgG (Cat.#20377), CF568 donkey anti-goat IgG (Cat.#20106, RRID: AB_10559672),
158 CF568 donkey anti-rabbit IgG (Cat.#20098, RRID: AB_10557118), and CF640T
159 donkey anti-goat IgG (Cat.#20179, RRID: AB_10853145).

160

161 *Whole.mount gut EdU assays.*

162 E12.5 or 14.5 pregnant females were injected intraperitoneally with
163 5-ethynyl-2'-deoxyuridine (EdU) (50 $\mu\text{g/g}$ body weight). Two hours after injection,
164 dissection of gut was followed by fixation and permeabilization in the same fashion as
165 whole-mount immunostaining. The preparations were washed twice for 3 min with 3%
166 BSA in PBS at room temperature. For EdU assays (Click.iT Plus EdU Imaging Kit,
167 Invitrogen), the reaction cocktail (reaction buffer, CuSO_4 , Alexa Flour 594 azide and
168 buffer additive as per manufacture's protocol) was added for 30 min followed by rinsing
169 twice for 3 min with 3% BSA in PBS in the dark at the room temperature. After EdU
170 labeling, whole-mount immunostaining was performed as described above.

171

172 *Cell counts*

173 Phox2b^+ neurons were counted on ten sections per investigated region of the gut at P0.
174 Phox2b^+ and EdU^+ Phox2b^+ ENS precursors were counted in a minimum of five areas
175 at even intervals of the midgut longitudinally (0.025 mm^2 each) and the rate of ENS
176 precursor proliferation was determined in animals for each genotype.

177

178 *Experimental design and statistical analysis*

179 Images were carefully selected to show the average effect obtained for each

180 experimental condition. All descriptive statistics are presented as means \pm SEM.
181 Normality of the data was tested with Levene's test (Dr.SPSS II Statistics software
182 (SPSS Inc, IL, USA)), and differences were subsequently assessed using unpaired t-test.
183 If assumptions for a parametric test were not met (Levene's test, $p < 0.05$), unpaired t
184 test with Welch correction was used. Statistical analyses for enteric neuron numbers
185 were performed using one-way ANOVA, followed by pairwise comparisons (Tukey's
186 *post hoc* test) where appropriate. GraphPad Prism 5 software (GraphPad Software Inc.
187 CA, USA) was used to conduct unpaired t-test with Welch correction, one-way ANOVA
188 with Tukey test and Chi-square test. Animals of both sex were used. No methods were
189 used for sample size determination.
190

191

192 **Results**193 **RET (C618F) enhances proliferation of ENS precursors and causes intestinal**
194 **hyperganglionosis**

195 To understand the biological impact of enhanced RET signaling on ENS development,
196 we examined mice expressing RET(C618F), a MEN2-associated RET-activating mutant.
197 Previous studies revealed that, among MEN2-associated RET mutants, those affecting
198 RET(C618) residues display moderate to low transforming activity in vitro
199 (Carlomagno et al., 1997; Ito et al., 1997). Our biochemical characterization indicated
200 that RET(C618F) displays slightly higher basal phosphorylation than normal and
201 requires GDNF for its full phosphorylation (Okamoto et al., 2019). Because
202 RET(C618F) retains GDNF-responsiveness and exhibits moderate activation of
203 RET-signaling, RET(C618F) is an ideal RET mutant to examine the effect of slight
204 RET-signaling enhancement on ENS development. Since mice expressing RET(C618F)
205 were engineered to express RET51(long isoform) cDNA carrying a C618F mutation by
206 the endogenous *Ret* promoter, the mutant allele is hereafter referred to as 51(C618F). As
207 a control, mice expressing wild type *RET51* cDNA were used (the allele referred to as
208 51). *Ret*^{51(C618F)/51(C618F)} mice were born apparently normally at an expected Mendelian
209 ratio but all died of unknown causes within 24 hours after birth (Okamoto et al., 2019).

210 In newborn (P0) *Ret*^{51(C618F)/51(C618F)} mice, histological analysis of the gut revealed that
211 the density of enteric neurons in the myenteric layer of the small intestine appeared
212 higher in *Ret*^{51(C618F)/51(C618F)} mice than *Ret*^{51/51} mice (control, Fig. 1A). Neuronal count
213 confirmed a significant increase in the numbers of myenteric neurons in both small
214 intestine and colon of *Ret*^{51(C618F)/51(C618F)} mice ($p < 0.0001$, Fig.1B).

215 We investigated proliferation of ENS precursors by anti-Phox2b staining (which detects
216 almost all ENS precursors during mid-gestation) combined with EdU labeling at
217 embryonic day 12.5 (E12.5: a period of ENS precursor migration) and E14.5 (a period
218 when ENS precursor migration is completed). This analysis revealed an increase in
219 double-positive cell populations in *Ret*^{51(C618F)/51(C618F)} embryos as compared to *Ret*^{51/51}
220 embryos in both of these developmental periods (Fig. 1C and D, *Ret*^{51(C618F)/51(C618F)} vs.
221 *Ret*^{51/51} in the midgut; 43.3±2.9% vs. 31.7±0.6% ($p = 0.019$) at E12.5 and 13.9±2.1% vs.
222 10.2±0.9% ($p = 0.046$) at E14.5, respectively). Thus, the increase in enteric neuron
223 numbers in newborn *Ret*^{51(C618F)/51(C618F)} mice is attributed at least in part to enhanced
224 proliferation of ENS progenitors

225 Previous studies suggested that reduced RET signaling impairs ENS migration (Young
226 et al., 2001; Natarajan et al., 2002; Uesaka et al., 2008) and that proliferation of ENS
227 precursors is a major driving force for ENS migration (Landman et al., 2007). We

228 therefore examined the migration of ENS precursors in *Ret*^{51(C618F)/51(C618F)} embryos.
229 Unexpectedly, the migratory wavefront of ENS precursors was always slightly delayed
230 in *Ret*^{51(C618F)/51(C618F)} embryos as compared to control embryos at E12.5 (Fig. 2, upper
231 panel). However, this delay was only transient and compensated for before birth. The
232 ENS was fully developed in all of *Ret*^{51(C618F)/51(C618F)} neonates (Fig. 2, lower panel).
233 In adult *Ret*^{51(C618F)/+} mice, we detected focal hyperplasia of thyroid C cells (Okamoto et
234 al., 2019), a pre-cancerous condition that leads to medullary thyroid carcinoma (Wolfe
235 et al., 1973). Together, these results indicate that, consistent with its enhanced activity in
236 vitro, RET51 (C618F) confers gain-of-function effects on development of the ENS and
237 thyroid C cells.

238

239 ***Ret*^{51(C618F)/-} mice display intestinal aganglionosis**

240 We moved on to examine the effects of a reduction in the dosage of the *RET* gene
241 because reduced RET expression is known to confer susceptibility to intestinal
242 aganglionosis in both human and mice (Emison et al., 2005; Uesaka et al., 2008). We
243 crossed *Ret*^{51/51} or *Ret*^{51(C618F)/51(C618F)} mice to *Ret*^{EGFP/+} mice in which one of the *Ret*
244 alleles was replaced by the *Ret-EGFP* allele (*Ret* null). Consistent with previous
245 observations that one allele of wild-type RET-expressing allele is sufficient for normal

246 development of the ENS in mice, the gut was fully furnished with ENS meshwork in
247 *Ret*^{51/EGFP} mice (Fig.3A and B left). In a stark contrast, all of *Ret*^{51(C618F)/EGFP} mice
248 displayed intestinal aganglionosis (Fig 3B). This result was surprising, as
249 *Ret*^{51(C618F)/51(C618F)} mice display hyperganglionosis (Fig.1A). Although the length of
250 aganglionic gut was varied, in about 62% of *Ret*^{51(C618F)/EGFP} mice (29 out of 34 mice
251 examined), the ENS was present only in the small intestine (Fig. 3C). Among these
252 mice, 8 mice (20% of all examined) displayed skip segment-type aganglionosis (Fig. 3B,
253 third picture). This skip segment appears to be developed at least partially due to
254 impaired migration of trans-mesenteric ENS progenitors, a cell population primarily
255 contributing to colonic ENS (Nishiyama et al., 2012), because we occasionally found a
256 limited number of enteric neurons scattered in the colon in some of *Ret*^{51(C618F)/EGFP}
257 embryos at E13.5, a period 2 days after trans-mesenteric migration is completed (Fig. 4).
258 These data demonstrate that *RET51(C618F)* allele causes severe intestinal aganglionosis
259 when the *RET* gene dosage is reduced to half.

260

261 **Premature neuronal differentiation impairs migration of ENS progenitors in**

262 ***Ret*^{51(C618F)/EGFP} embryos**

263 To investigate the mechanism underlying the impaired ENS development in

264 *Ret*^{51(C618F)/EGFP} mice, we conducted whole-mount immunohistochemical analyses of
265 embryonic gut (E12.5). In control (*Ret*^{51/EGFP}) embryos, ENS progenitors at the
266 migrating wavefront invaded the proximal colon and expressed both RET (revealed by
267 GFP fluorescence) and Sox10 (Fig. 5A, left), indicating those cells are immature
268 progenitors. Consistent with this expression pattern, none of the cells at the wavefront
269 expressed PGP9.5 (Fig. 5B, left), a marker for neuronal differentiation. In contrast, in
270 *Ret*^{51(C618F)/EGFP} embryos, Sox10 expression was lost in many cells at the wavefront (Fig.
271 5A, right, arrowheads). Associated with this change, we found aberrant expression of
272 PGP9.5 in ENS progenitors at the migratory wavefront, which was located primarily in
273 the midgut (Fig. 5B, right). These results indicate that premature neuronal
274 differentiation is induced in ENS progenitors at the migratory wavefront in
275 *Ret*^{51(C618F)/EGFP} embryos.

276 A previous study revealed that elevation of ERK activity is associated with induction of
277 neuronal differentiation in ENS progenitors (Uesaka et al., 2013). We examined ERK
278 activation by whole-mount staining of embryonic gut (E12.5) using anti-phospho Erk
279 (pErk) antibodies. In *Ret*^{51/EGFP} embryos, pErk-positive ENS progenitors were abundant
280 in proximal regions of the midgut, whereas such cells were almost undetectable at the
281 wavefront region (Fig. 4C, right upper panels). In contrast, pErk-positive cells were

282 frequently observed not only in the proximal midgut but also in the wavefront regions in
283 *Ret*^{51(C618F)/EGFP} embryos (Fig. 5C, left and right bottom panels). These data collectively
284 indicate that single allele-only expression of RET51 (C618F) causes premature enteric
285 neuronal differentiation in vivo.

286

287 **GDNF-mediated activation of RET51(C618F) is responsible for premature**
288 **neuronal differentiation of ENS progenitors**

289 Previous biochemical analyses revealed that RET51(C618F) responds to GDNF and
290 displays enhanced phosphorylation in vitro. To investigate whether GDNF-induced
291 stimulation of RET51(C618F) contributes to severe aganglionosis phenotype in
292 *Ret*^{51(C618F)/+} mice, we examined whether severity of the phenotype changes in
293 *Ret*^{51(C618F)/EGFP} mice on *Gdnf*^{+/-} background. By whole-mount GFP staining of the
294 neonatal gut (n= 20), we found that most of *Ret*^{51(C618F)/EGFP} /*Gdnf*^{+/-} mice (80%)
295 displayed colonic aganglionosis (Fig. 6A), which stood in a sharp contrast to the ENS
296 phenotype of *Ret*^{51(C618F)/EGFP} that showed mostly extensive aganglionosis (aganglionic
297 segment exceeding to the small intestine). Chi- square test of independence confirmed
298 the significant differences between *Ret*^{51(C618F)/EGFP} /*Gdnf*^{+/-} and *Ret*^{51(C618F)/EGFP}
299 /*Gdnf*^{+/+} mice ($p = 0.005 < 0.01$). Interestingly, in one case, the ENS was found fully

300 developed up to the anal end (Fig. 6B). Moreover, skip segment-type aganglionosis,
301 which was identified in 24% of $Ret^{51(C618F)/-}$ mice, was not detected in any of
302 $Ret^{51(C618F)/EGFP}/Gdnf^{+/-}$ mice. These results collectively indicate that reduction in
303 GDNF levels exerts significant rescue effects on severe aganglionosis phenotype (Fig.
304 6A-B).

305 At E12.5, migration of ENS precursors was delayed in $Ret^{51(C618F)/EGFP}/Gdnf^{+/-}$ embryos
306 as compared to $Ret^{51/EGFP}/Gdnf^{+/-}$ embryos (Fig. 6C). To examine the effect of the
307 reduction of *Gdnf* gene dosage on intracellular signaling, whole-mount pERK staining
308 was performed on the gut of $Ret^{51(C618F)/EGFP}/Gdnf^{+/-}$ embryos (E12.5). Similar to wild
309 type or $Ret^{51/EGFP}$ embryos (Fig. 4C top), ERK phosphorylation was undetectable at the
310 wavefront regions of $Ret^{51(C618F)/EGFP}/Gdnf^{+/-}$ embryos (Fig. 6D, right). These data reveal
311 that GDNF-mediated activation of RET51(C618F) is responsible for aberrant
312 phosphorylation of ERK in ENS precursors at the wavefront and causes intestinal
313 aganglionosis in $Ret^{51(C618F)/-}$ embryos.

314

315 **An allelic loss of the *Ednrb* gene exacerbates the ENS phenotype of $Ret^{51(C618F)/-}$**

316 **mice**

317 Previous studies revealed a genetic interaction between the *Ret* and *Ednrb* genes in

318 HSCR pathogenesis. Either *Ret* heterozygosity or the *Ednrb* *ls/ls* allele alone exerts no
319 adverse effect on ENS development, but induces severe intestinal aganglionosis when
320 combined (Carrasquillo et al., 2002). *Ednrb* signaling regulates multiple processes of
321 ENS development including migration, proliferation and differentiation of ENS
322 precursors (Barlow et al., 2003; Kruger et al., 2003). We examined a potential genetic
323 interaction between the *Ret*^{51(C618F)} allele and the *Ednrb* gene by crossing
324 *Ret*^{51/51(C618F)} mice to *Ednrb*^{+/-}/*Ret*^{EGFP/+} mice. We found that, in contrast to
325 *Ret*^{51/EGFP}/*Ednrb*^{+/-} embryos, which displayed normal ENS development,
326 *Ret*^{51(C618F)/EGFP} / *Ednrb*^{+/-} embryos exhibited severe intestinal aganglionosis in which
327 the ENS is observed only in the proximal part of the small intestine (Fig. 7A-C).
328 Immunohistochemical examination of ENS precursors revealed robust phosphorylation
329 of ERK and loss of Sox10 expression at the wavefront regions (Fig. 7D). Thus reduction
330 of one copy of the *Ednrb* gene leads to exacerbation of the aganglionosis phenotype,
331 which contrasted the ameliorating effect by the reduction of the *Gdnf* gene dosage. This
332 difference is not caused by the differential expression levels of GFR α 1, the cognate
333 receptor for GDNF involved in HSCR pathogenesis (Lui et al., 2002), as it was
334 expressed at comparable levels in *Gdnf*^{+/-}, *Ednrb*^{+/-} and wild type embryos (Fig. 7E). At
335 any rate, these results reveal a clear genetic interaction between the *Ret*^{51(C618F)} allele

336 and the *Ednrb* gene and suggest that the Ednrb signaling functions to inhibit premature

337 differentiation of ENS precursors in this context.

338

339

340 **Discussion**

341 In this study, we have provided evidence that RET(C618F), a RET-activating
342 mutant, causes intestinal aganglionosis when the *Ret* gene copy number is reduced to
343 half, which is contrary to the current consensus that enteric aganglionosis is caused by
344 inactivating RET mutations. This unexpected finding provides novel insights into
345 mechanisms underlying the development of the ENS by RET/GDNF signaling and the
346 pathogenesis of HSCR.

347 The involvement of RET activating mutations in HSCR was first described in
348 co-segregation of MEN2A/FMTC and HSCR in a fraction of families. These patients
349 carry missense mutations in the *RET* gene, which substitutes arginine or serine for a
350 cysteine residue at position 618 or 620. These RET mutants display ligand-independent
351 constitutive activation due to inter-molecular di-sulfide-linked dimerization (Santoro et
352 al., 1995) and simultaneously loses cell surface expression (Asai et al., 1995). The
353 former property contributes to neoplastic pathology including MTC and
354 pheochromocytoma, whereas the latter contributes to impaired development of the ENS
355 (HSCR). Therefore, in the context of ENS development, these mutants (C618R, C618S
356 and C620R) behave as RET-inactivating mutants (Mulligan et al., 1994; Borst et al.,
357 1995). Animal studies support this notion, as mice harboring RET(C620R) mutation in a

358 homozygous fashion display kidney agenesis and intestinal aganglionosis, a phenotype
359 identical to that of *Ret*-deficient mice (Carniti et al., 2006; Yin et al., 2007).
360 RET(C618F) examined in this study exhibited distinct properties. Unlike other C618 or
361 C620 mutants, RET(C618F) is expressed on the cell surface (Okamoto et al., 2019).
362 Although phosphorylation levels of RET(C618F) are slightly higher than those of wild
363 type RET, GDNF stimulation further enhances phosphorylation of RET(C618F)
364 (Okamoto et al., 2019). Thus, RET(C618F) is a GDNF-responsive RET-activating
365 mutant. Consistent with these biochemical properties, *Ret*^{51(C618F)/51(C618F)} mice had
366 increased numbers of enteric neurons due to enhanced proliferation of ENS precursors.
367 Surprisingly, despite the activating nature of RET51(C618F), *Ret*^{51(C618F)/-} mice
368 displayed severe intestinal aganglionosis, in sharp contrast to *Ret*^{RET51/-} mice (control),
369 which exhibited no ENS deficit. This study provides evidence, for the first time to our
370 knowledge, that RET-activating mutations can cause intestinal aganglionosis when
371 coupled with a reduction in the *Ret* gene dosage.

372 It is important to note that, the *RET C618F* allele displays genetic interaction
373 with the *Ednrb* gene, which is known as a modifier gene for HSCR carrying mutations
374 in the *RET* gene. Our findings suggest a novel pathogenetic mechanisms of HSCR by
375 revealing how reduced RET expression affects ENS development and confers

376 susceptibility to HSCR (Emison et al., 2005). It is also important to note that many of
377 *Ret*^{51(C618F)/-} mice displayed skip-segment aganglionosis. *Ret*^{51(C618F)/-} mice thus serve as
378 the first valuable platform to investigate the molecular and cellular mechanisms
379 underlying this mysterious condition.

380 Histological examination of *Ret*^{51(C618F)/-} embryos revealed that premature
381 neuronal differentiation of ENS precursors is likely to be the cause of the intestinal
382 aganglionosis. Exacerbation of the aganglionic phenotype by the reduction of the *Ednrb*
383 gene supports this possibility because endothelin-3/*Ednrb* signaling prevents premature
384 neuronal differentiation (Wu et al., 1999). The aganglionic phenotype of *Ret*^{51(C618F)/-}
385 embryos stands in sharp contrast to that of *Ret*^{51(C618F)/51(C618F)} embryos, in which ENS
386 precursors underwent proliferation rather than differentiation. Although the exact
387 mechanism by which ENS precursors adopt to a different cell fate (proliferation or
388 differentiation) is unknown, it may involve regulation of Erk phosphorylation. In PC12
389 cells, EGF treatment enhances cell proliferation, while FGF treatment induces neuronal
390 differentiation. This difference in cell fate is tightly associated with the levels and
391 kinetics of Erk phosphorylation. EGF evokes a rapid surge and subsequent abrupt
392 quenching of Erk phosphorylation, whereas FGF induces long-lasting and moderate
393 levels of Erk phosphorylation (Qiu and Green, 1991; Traverse et al., 1992; Nguyen et al.,

394 1993). Interestingly, Erk phosphorylation-associated cell fate determination in ENS
395 precursors was reported previously (Natarajan et al., 2002; Asai et al., 2006; Goto et al.,
396 2013) . We can therefore assume that Erk activity is differentially regulated in ENS
397 precursors between *Ret*^{51(C618F)/51(C618F)} and *Ret*^{51(C618F)/-} embryos. We tried to examine
398 this possibility by culturing ENS precursors and conducting biochemical analyses.
399 Unfortunately, however, *Ret*^{51(C618F)/-} ENS precursors displayed a tendency to
400 differentiate in vitro, and we were unable to obtain reliable data. To understand the
401 mechanisms underlying the intestinal aganglionosis in *Ret*^{51(C618F)/-} mice, we also have
402 to understand the biochemical properties of RET51(C618F) in more detail. Although
403 RET51(C618F) is expressed on cell surface, it is also detected in the cytoplasm
404 (Okamoto et al., 2019). The latter likely reflects localization in ER, which is commonly
405 observed in all MEN-associated RET mutant proteins (Wagner et al., 2012). Thus,
406 RET51(C618F) has combined properties of wild type RET and MEN-associated RET
407 mutants. Even on the cell surface, it is unknown whether RET51(C618F) behaves as
408 wild type RET. For instance, upon GDNF binding to GFR α receptors, wild type RET
409 protein gets recruited to the raft and phosphorylated, which provides a platform to
410 activate Src and Akt-PI3 kinase efficiently. It is currently unknown how RET51(C618F)
411 is localized and activates intracellular signaling molecules on the cell surface. In these

412 respects, RET51(C618F) may not reflect enhanced activity of purely wild type RET.
413 RET51(C618F) has unique biochemical properties among MEN-associated RET
414 mutants, which suggest that all of RET-activating mutations do not necessarily cause the
415 intestinal aganglionosis by *RET* gene dosage reduction.

416 Amelioration of the phenotype in *Ret*^{51(C618F)/-} embryos by the *Gdnf* gene
417 reduction indicates that GDNF-mediated activation of RET51(C618F) is responsible for
418 the severe aganglionic phenotype. Although NRTN also activates RET in developing
419 ENS (Heuckeroth et al., 1998), contribution of NRTN-mediated RET(C618F) activation
420 to the aganglionic phenotype is unlikely because expression of GFR α 2, the cognate
421 receptor for NRTN, occurs later than a period when the aganglionic phenotype in
422 *Ret*^{51(C618F)/-} embryos becomes obvious. It is important to note that, in normal ENS
423 development, enteric neuron numbers are determined primarily by the levels of GDNF
424 signaling. Mice heterozygous for the GDNF-deficient allele (*Gdnf*^{+/-} mice) display
425 reduced numbers of enteric neurons (Gianino et al., 2003). In contrast, reduction of
426 Sprouty2, an inhibitor of Erk phosphorylation downstream of RET/GDNF signaling,
427 leads to hyperganglionosis of the gut (Taketomi et al., 2005). This hyperganglionosis
428 phenotype is suppressed on *Gdnf*^{+/-} background. Evidence also suggests that RET
429 expression is regulated by RET activity induced by GDNF (Oppenheim et al., 2000).

430 Taken together, both signaling and expression of RET are exquisitely controlled by the
431 availability of GDNF, Sprouty2 and phosphor-Erk. Even a slight disturbance (both
432 upregulation and downregulation) of RET signaling can abrogate ENS development
433 (Nagy et al., 2020). Understanding the development and developmental disorders of the
434 ENS requires the elucidation of interactions among these molecules.
435

436

437 **References**

438 Airaksinen MS, Saarma M (2002) The GDNF family: signalling, biological functions

439 and therapeutic value. *Nat Rev Neurosci* 3:383-394.

440 Amiel J et al. (2008) Hirschsprung disease, associated syndromes and genetics: a review.

441 *Journal of medical genetics* 45:1-14.

442 Asai N, Iwashita T, Matsuyama M, Takahashi M (1995) Mechanism of activation of the

443 ret proto-oncogene by multiple endocrine neoplasia 2A mutations. *Molecular*

444 and cellular biology 15:1613-1619.

445 Asai N, Fukuda T, Wu Z, Enomoto A, Pachnis V, Takahashi M, Costantini F (2006)

446 Targeted mutation of serine 697 in the Ret tyrosine kinase causes migration

447 defect of enteric neural crest cells. *Development (Cambridge, England)*

448 133:4507-4516.

449 Baloh RH, Enomoto H, Johnson EM, Jr., Milbrandt J (2000) The GDNF family ligands

450 and receptors - implications for neural development. *Curr Opin Neurobiol*

451 10:103-110.

452 Barlow A, de Graaff E, Pachnis V (2003) Enteric nervous system progenitors are

453 coordinately controlled by the G protein-coupled receptor EDNRB and the

454 receptor tyrosine kinase RET. *Neuron* 40:905-916.

- 455 Borst MJ, VanCamp JM, Peacock ML, Decker RA (1995) Mutational analysis of
456 multiple endocrine neoplasia type 2A associated with Hirschsprung's disease.
457 *Surgery* 117:386-391.
- 458 Carlomagno F, Salvatore G, Cirafici AM, De Vita G, Melillo RM, de Franciscis V,
459 Billaud M, Fusco A, Santoro M (1997) The different RET-activating capability
460 of mutations of cysteine 620 or cysteine 634 correlates with the multiple
461 endocrine neoplasia type 2 disease phenotype. *Cancer research* 57:391-395.
- 462 Carniti C, Belluco S, Riccardi E, Cranston AN, Mondellini P, Ponder BA, Scanziani E,
463 Pierotti MA, Bongarzone I (2006) The Ret(C620R) mutation affects renal and
464 enteric development in a mouse model of Hirschsprung's disease. *The American*
465 *journal of pathology* 168:1262-1275.
- 466 Carrasquillo MM, McCallion AS, Puffenberger EG, Kashuk CS, Nouri N, Chakravarti A
467 (2002) Genome-wide association study and mouse model identify interaction
468 between RET and EDNRB pathways in Hirschsprung disease. *Nature genetics*
469 32:237-244.
- 470 Druckenbrod NR, Powers PA, Bartley CR, Walker JW, Epstein ML (2008) Targeting of
471 endothelin receptor-B to the neural crest. *Genesis* 46:396-400.
- 472 Edery P, Lyonnet S, Mulligan LM, Pelet A, Dow E, Abel L, Holder S, Nihoul-Fekete C,

- 473 Ponder BA, Munnich A (1994) Mutations of the RET proto-oncogene in
474 Hirschsprung's disease. *Nature* 367:378-380.
- 475 Emison ES, McCallion AS, Kashuk CS, Bush RT, Grice E, Lin S, Portnoy ME, Cutler
476 DJ, Green ED, Chakravarti A (2005) A common sex-dependent mutation in a
477 RET enhancer underlies Hirschsprung disease risk. *Nature* 434:857-863.
- 478 Gianino S, Grider JR, Cresswell J, Enomoto H, Heuckeroth RO (2003) GDNF
479 availability determines enteric neuron number by controlling precursor
480 proliferation. *Development (Cambridge, England)* 130:2187-2198.
- 481 Goto A, Sumiyama K, Kamioka Y, Nakasyo E, Ito K, Iwasaki M, Enomoto H, Matsuda
482 M (2013) GDNF and endothelin 3 regulate migration of enteric neural
483 crest-derived cells via protein kinase A and Rac1. *J Neurosci* 33:4901-4912.
- 484 Hansford JR, Mulligan LM (2000) Multiple endocrine neoplasia type 2 and RET: from
485 neoplasia to neurogenesis. *Journal of medical genetics* 37:817-827.
- 486 Heuckeroth RO, Lampe PA, Johnson EM, Milbrandt J (1998) Neurturin and GDNF
487 promote proliferation and survival of enteric neuron and glial progenitors in
488 vitro. *Developmental biology* 200:116-129.
- 489 Ito S, Iwashita T, Asai N, Murakami H, Iwata Y, Sobue G, Takahashi M (1997)
490 Biological properties of Ret with cysteine mutations correlate with multiple

- 491 endocrine neoplasia type 2A, familial medullary thyroid carcinoma, and
492 Hirschsprung's disease phenotype. *Cancer research* 57:2870-2872.
- 493 Jain S, Encinas M, Johnson EM, Jr., Milbrandt J (2006) Critical and distinct roles for
494 key RET tyrosine docking sites in renal development. *Genes & development*
495 20:321-333.
- 496 Kapoor A, Jiang Q, Chatterjee S, Chakraborty P, Sosa MX, Berrios C, Chakravarti A
497 (2015) Population variation in total genetic risk of Hirschsprung disease from
498 common RET, SEMA3 and NRG1 susceptibility polymorphisms. *Human*
499 *molecular genetics* 24:2997-3003.
- 500 Kruger GM, Mosher JT, Tsai YH, Yeager KJ, Iwashita T, Garipey CE, Morrison SJ
501 (2003) Temporally distinct requirements for endothelin receptor B in the
502 generation and migration of gut neural crest stem cells. *Neuron* 40:917-929.
- 503 Landman KA, Simpson MJ, Newgreen DF (2007) Mathematical and experimental
504 insights into the development of the enteric nervous system and Hirschsprung's
505 disease. *Development, growth & differentiation* 49:277-286.
- 506 Lewandoski M, Meyers EN, Martin GR (1997) Analysis of Fgf8 gene function in
507 vertebrate development. *Cold Spring Harb Symp Quant Biol* 62:159-168.
- 508 Lui VC, Samy ET, Sham MH, Mulligan LM, Tam PK (2002) Glial cell line-derived

- 509 neurotrophic factor family receptors are abnormally expressed in aganglionic
510 bowel of a subpopulation of patients with Hirschsprung's disease. *Lab Invest*
511 82:703-712.
- 512 Margraf RL, Crockett DK, Krautscheid PM, Seamons R, Calderon FR, Wittwer CT,
513 Mao R (2009) Multiple endocrine neoplasia type 2 RET protooncogene
514 database: repository of MEN2-associated RET sequence variation and reference
515 for genotype/phenotype correlations. *Human mutation* 30:548-556.
- 516 Moore MW, Klein RD, Farinas I, Sauer H, Armanini M, Phillips H, Reichardt LF, Ryan
517 AM, Carver-Moore K, Rosenthal A (1996) Renal and neuronal abnormalities in
518 mice lacking GDNF. *Nature* 382:76-79.
- 519 Mulligan LM, Eng C, Attie T, Lyonnet S, Marsh DJ, Hyland VJ, Robinson BG, Frilling
520 A, Verellen-Dumoulin C, Safar A, et al. (1994) Diverse phenotypes associated
521 with exon 10 mutations of the RET proto-oncogene. *Human molecular genetics*
522 3:2163-2167.
- 523 Nagy N, Guyer RA, Hotta R, Zhang D, Newgreen DF, Halasy V, Kovacs T, Goldstein
524 AM (2020) RET overactivation leads to concurrent Hirschsprung disease and
525 intestinal ganglioneuromas. *Development (Cambridge, England)* 147.
- 526 Natarajan D, Marcos-Gutierrez C, Pachnis V, de Graaff E (2002) Requirement of

- 527 signalling by receptor tyrosine kinase RET for the directed migration of enteric
528 nervous system progenitor cells during mammalian embryogenesis.
529 *Development* (Cambridge, England) 129:5151-5160.
- 530 Nguyen TT, Scimeca JC, Filloux C, Peraldi P, Carpentier JL, Van Obberghen E (1993)
531 Co-regulation of the mitogen-activated protein kinase, extracellular
532 signal-regulated kinase 1, and the 90-kDa ribosomal S6 kinase in PC12 cells.
533 Distinct effects of the neurotrophic factor, nerve growth factor, and the
534 mitogenic factor, epidermal growth factor. *The Journal of biological chemistry*
535 268:9803-9810.
- 536 Nishiyama C, Uesaka T, Manabe T, Yonekura Y, Nagasawa T, Newgreen DF, Young
537 HM, Enomoto H (2012) Trans-mesenteric neural crest cells are the principal
538 source of the colonic enteric nervous system. *Nature neuroscience*
539 15:1211-1218.
- 540 Okamoto M, Yoshioka Y, Maeda K, Bito Y, Fukumoto T, Uesaka T, Enomoto H (2019)
541 Mice conditionally expressing RET(C618F) mutation display C cell hyperplasia
542 and hyperganglionosis of the enteric nervous system. *Genesis* 57:e23292.
- 543 Oppenheim RW, Houenou LJ, Parsadanian AS, Prevet D, Snider WD, Shen L (2000)
544 Glial cell line-derived neurotrophic factor and developing mammalian

- 545 motoneurons: regulation of programmed cell death among motoneuron subtypes.
546 J Neurosci 20:5001-5011.
- 547 Qiu MS, Green SH (1991) NGF and EGF rapidly activate p21ras in PC12 cells by
548 distinct, convergent pathways involving tyrosine phosphorylation. Neuron
549 7:937-946.
- 550 Romeo G, Ronchetto P, Luo Y, Barone V, Seri M, Ceccherini I, Pasini B, Bocciardi R,
551 Lerone M, Kaariainen H, et al. (1994) Point mutations affecting the tyrosine
552 kinase domain of the RET proto-oncogene in Hirschsprung's disease. Nature
553 367:377-378.
- 554 Santoro M, Carlomagno F, Romano A, Bottaro DP, Dathan NA, Grieco M, Fusco A,
555 Vecchio G, Matoskova B, Kraus MH, et al. (1995) Activation of RET as a
556 dominant transforming gene by germline mutations of MEN2A and MEN2B.
557 Science 267:381-383.
- 558 Taketomi T, Yoshiga D, Taniguchi K, Kobayashi T, Nonami A, Kato R, Sasaki M,
559 Sasaki A, Ishibashi H, Moriyama M, Nakamura K, Nishimura J, Yoshimura A
560 (2005) Loss of mammalian Sprouty2 leads to enteric neuronal hyperplasia and
561 esophageal achalasia. Nature neuroscience 8:855-857.
- 562 Tilghman JM, Ling AY, Turner TN, Sosa MX, Krumm N, Chatterjee S, Kapoor A, Coe

- 563 BP, Nguyen KH, Gupta N, Gabriel S, Eichler EE, Berrios C, Chakravarti A
564 (2019) Molecular Genetic Anatomy and Risk Profile of Hirschsprung's Disease.
565 The New England journal of medicine 380:1421-1432.
- 566 Tomuschat C, Puri P (2015) RET gene is a major risk factor for Hirschsprung's disease:
567 a meta-analysis. Pediatric surgery international 31:701-710.
- 568 Traverse S, Gomez N, Paterson H, Marshall C, Cohen P (1992) Sustained activation of
569 the mitogen-activated protein (MAP) kinase cascade may be required for
570 differentiation of PC12 cells. Comparison of the effects of nerve growth factor
571 and epidermal growth factor. Biochem J 288 (Pt 2):351-355.
- 572 Uesaka T, Nagashimada M, Enomoto H (2013) GDNF signaling levels control
573 migration and neuronal differentiation of enteric ganglion precursors. J Neurosci
574 33:16372-16382.
- 575 Uesaka T, Nagashimada M, Yonemura S, Enomoto H (2008) Diminished Ret expression
576 compromises neuronal survival in the colon and causes intestinal aganglionosis
577 in mice. The Journal of clinical investigation 118:1890-1898.
- 578 Wagner SM, Zhu S, Nicolescu AC, Mulligan LM (2012) Molecular mechanisms of RET
579 receptor-mediated oncogenesis in multiple endocrine neoplasia 2. Clinics (Sao
580 Paulo) 67 Suppl 1:77-84.

- 581 Wells SA, Jr., Pacini F, Robinson BG, Santoro M (2013) Multiple endocrine neoplasia
582 type 2 and familial medullary thyroid carcinoma: an update. *The Journal of*
583 *clinical endocrinology and metabolism* 98:3149-3164.
- 584 Wolfe HJ, Melvin KE, Cervi-Skinner SJ, Saadi AA, Juliar JF, Jackson CE, Tashjian AH,
585 Jr. (1973) C-cell hyperplasia preceding medullary thyroid carcinoma. *The New*
586 *England journal of medicine* 289:437-441.
- 587 Wu JJ, Chen JX, Rothman TP, Gershon MD (1999) Inhibition of in vitro enteric
588 neuronal development by endothelin-3: mediation by endothelin B receptors.
589 *Development (Cambridge, England)* 126:1161-1173.
- 590 Yin L, Puliti A, Bonora E, Evangelisti C, Conti V, Tong WM, Medard JJ, Lavoue MF,
591 Forey N, Wang LC, Manie S, Morel G, Raccurt M, Wang ZQ, Romeo G (2007)
592 C620R mutation of the murine ret proto-oncogene: loss of function effect in
593 homozygotes and possible gain of function effect in heterozygotes. *Int J Cancer*
594 121:292-300.
- 595 Young HM, Hearn CJ, Farlie PG, Canty AJ, Thomas PQ, Newgreen DF (2001) GDNF is
596 a chemoattractant for enteric neural cells. *Developmental biology* 229:503-516.
597
598

599

600 **Figure legends**

601 **Figure 1.** $Ret^{51(C618F)/51(C618F)}$ mice display hypertrophy of enteric ganglia

602 A, Whole-mount Phox2b staining (green) of enteric neurons in the myenteric plexus of
603 the small intestine from P0 $Ret^{+/+}$, $Ret^{51/51}$, and $Ret^{51(C618F)/51(C618F)}$ mice. **B,**
604 Quantification of Phox2b⁺ enteric neuron numbers in the small intestine and the colon
605 from P0 $Ret^{+/+}$ (n=3), $Ret^{51/51}$ (n=3), and $Ret^{51(C618F)/51(C618F)}$ (n=6) mice. * $p = 0.001$, ** p
606 <0.0001 , one-way ANOVA with Tukey's *post hoc* test. **C,D,** Detection of EdU
607 (magenta) incorporated into Phox2b⁺ ENS precursors (green) in the midgut from E12.5
608 (C) and E14.5 (D) $Ret^{51/51}$ and $Ret^{51(C618F)/51(C618F)}$ fetuses. The gut was labeled by a
609 two-hour pulse of EdU. The graphs (right panels) display the rate of ENS precursor
610 proliferation at E12.5 and 14.5 $Ret^{51/51}$ (n=3) and $Ret^{51(C618F)/51(C618F)}$ (n=3) fetuses. * p
611 <0.05 , unpaired t-test. Scale bars: **A**, 50 μm ; **C, D**, 20 μm .

612

613 **Figure 2.** $Ret^{51(C618F)/51(C618F)}$ mice exhibit complete gut colonization by ENS precursors

614 Phox2b-labeled ENS precursors and neurons (green) in the developing gut in $Ret^{51/51}$
615 and $Ret^{51(C618F)/51(C618F)}$ mice at E12.5 (upper panels) and P0 (lower panels). Migration
616 of ENS precursors is slightly delayed at E12.5, but gut colonization by them is

617 completed at P0. Arrowheads depict the front of the migrating ENS precursors. Ce,
618 cecum; Co, colon; Si, small intestine; Hg, hindgut, Mg, midgut. Scale bars: 250 μ m
619 (upper panels); 500 μ m (lower panels).

620

621 **Figure 3.** *Ret*^{51(C618F)/-} mice exhibit intestinal aganglionosis.

622 **A,B,** Whole-mount images of the enteric neurons stained with anti-PGP-9.5 (A) or
623 labeled by GFP (B) in P0 *Ret*^{51/+} and *Ret*^{51(C618F)/+}, *Ret*^{51/EGFP}, and *Ret*^{51(C618F)/EGFP} gut.

624 Complete gut colonization by ENS cells was seen in *Ret*^{51/+}, *Ret*^{51(C618F)/+} and *Ret*^{51/EGFP}

625 mice (white arrowheads), while *Ret*^{51(C618F)/EGFP} mice exhibited disrupted colonization

626 of the gut by ENCCs. The wavefront (yellow arrowheads) was defined as the most

627 caudal continuous strands of EGFP⁺ cells. Some *Ret*^{51(C618F)/EGFP} mice show skip

628 segment aganglionosis where small regions of the colon contain enteric ganglia (white

629 dotted region). **C,** The proportion of three types of aganglionic phenotype (small

630 intestinal, skip segment and colonic aganglionosis). Ce, cecum; Co, colon; Si, small

631 intestine. Scale bars: **A-B,** 1 mm.

632

633 **Figure 4.** Detection of a few enteric neurons in the hindgut of *Ret*^{51(C618F)/EGFP} embryos.

634 Whole mount preparation of embryonic gut showing the presence of a few

635 differentiating enteric neurons (A, inset) revealed by anti-PGP9.5 antibody (B). Scale
636 bars: **A**, 100 μm ; **B**, 50 μm .

637

638

639 **Figure 5.** Reduced RET51(C618) expression leads to premature differentiation of ENS
640 precursors at the migratory wavefront.

641 **A**, Whole-mount images of GFP-labeled cells in the gut from E12.5 *Ret*^{51/EGFP} and
642 *Ret*^{51(C618F)/EGFP} embryos (left panels). GFP⁺ cells in the migratory wavefront were
643 stained by anti-Sox10 (right panels), whereas Sox10-negative GFP⁺ cells (white
644 arrowheads) were found at the delayed migratory wavefront (open arrowhead) of
645 *Ret*^{51(C618F)/EGFP} gut. **B**, Whole-mount images of GFP-labeled cells stained with
646 anti-PGP9.5 in E12.5 *Ret*^{51/EGFP} and *Ret*^{51(C618F)/EGFP} gut. PGP9.5-labeled GFP⁺ cells
647 were detected at the delayed migratory wavefront of *Ret*^{51(C618F)/EGFP} gut. **C**,
648 Immunohistochemical staining for GFP (green), Sox10 (blue) and activated ERK
649 (pERK, magenta) in ENS cells of *Ret*^{51/EGFP} and *Ret*^{51(C618F)/EGFP} embryos at E12.5. In
650 the migratory wavefront of *Ret*^{51(C618F)/EGFP} embryos, pERK was mainly observed in
651 GFP⁺ and Sox10⁻ differentiating neurons (white arrowheads). Hg, hindgut; Mg, midgut;
652 Ro, rostral; Ca, caudal. Scale bars: **A**, 250 μm ; **B**, 25 μm ; **C**, 20 μm .

653

654 **Figure 6.** Reducing *Gdnf* gene dosage moderately rescues ENS phenotype of
655 *Ret*^{51(C618F)/-} mice.

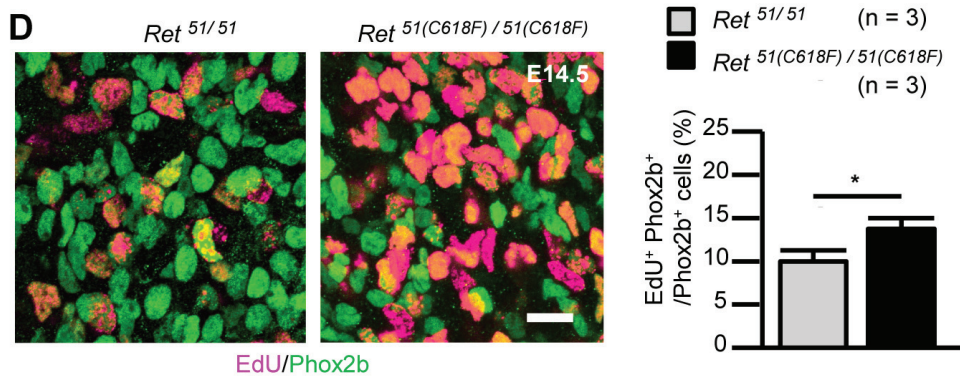
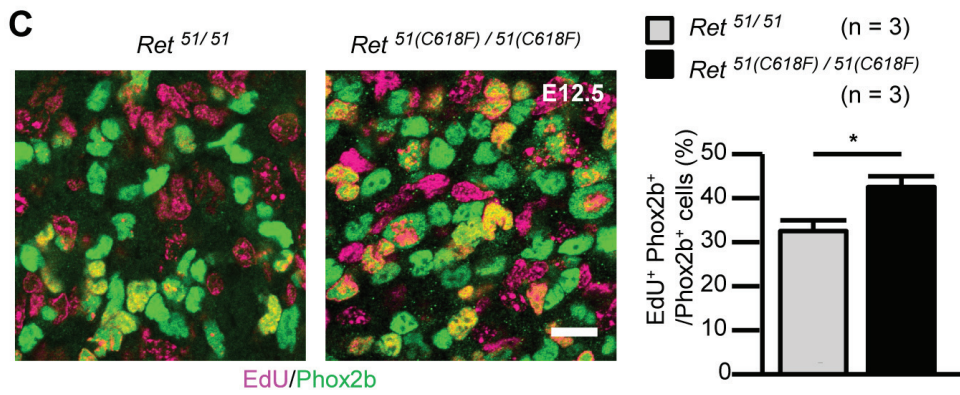
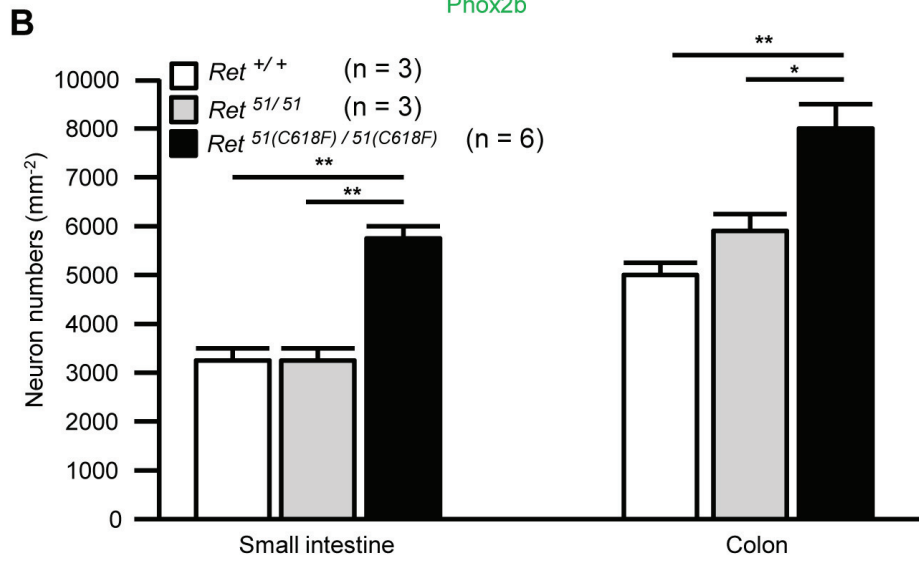
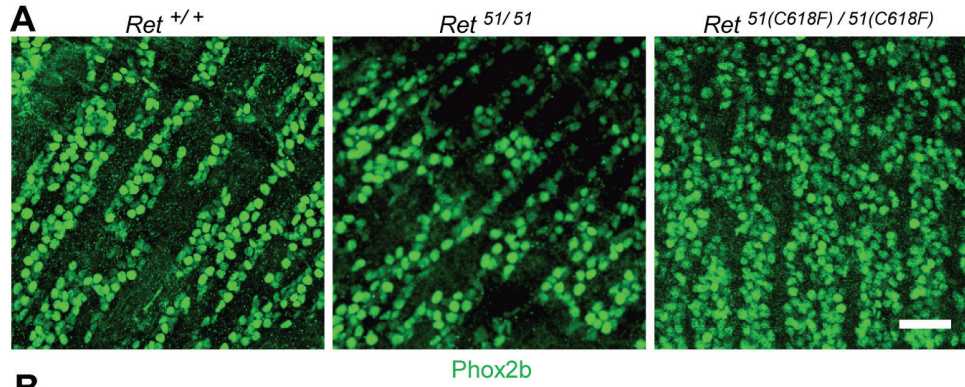
656 **A,** Representative images of P0 *Ret*^{51/EGFP}/*Gdnf*^{+/-} and *Ret*^{51(C618F)/EGFP}/*Gdnf*^{+/-} large
657 intestine showing complete colonization with GFP-positive enteric neurons. **B,**
658 Comparison of ENS wavefront location between *Ret*^{51(C618F)/EGFP} and *Ret*^{51(C618F)/EGFP}/
659 *Gdnf*^{+/-} mice at P0. Reduction of *Gdnf* gene dosage significantly ameliorated the
660 severity of enteric aganglionosis (chi-square test, $p < 0.01$). **C,** Representative images of
661 E12.5 *Ret*^{51/EGFP}/*Gdnf*^{+/-} and *Ret*^{51(C618F)/EGFP}/*Gdnf*^{+/-} gut displaying colonization by
662 GFP-positive ENS precursors. White arrowheads indicate the location of ENS precursor
663 wavefront. **D,** Whole-mount GFP, Sox10 and pERK pathway stainings of ENS cells of
664 *Ret*^{51(C618F)/EGFP}/*Gdnf*^{+/-} embryos at E12.5. Activation of ERK was not observed in ENS
665 precursors at the migratory wavefront. Ce, cecum; Co, colon; Si, small intestine; Hg,
666 hindgut; Mg, midgut. Scale bars: **A,** 1000 μm ; **C,** 250 μm ; **D,** 20 μm .

667

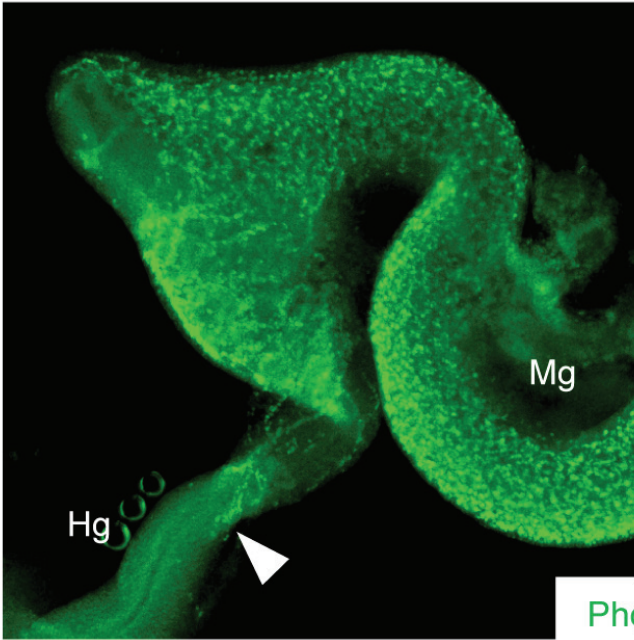
668 **Figure 7.** The severity of interruption of the ENS migration depends on the *Ednrb* gene
669 dosage in *RET*^{51(C618F)/-} mice.

670 **A,** Whole-mount GFP staining of P0 *Ret*^{51/EGFP}/*Ednrb*^{+/-} and *Ret*^{51(C618F)/EGFP}/*Ednrb*^{+/-}

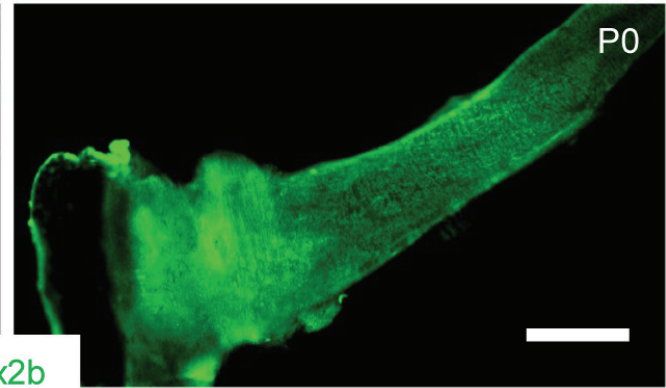
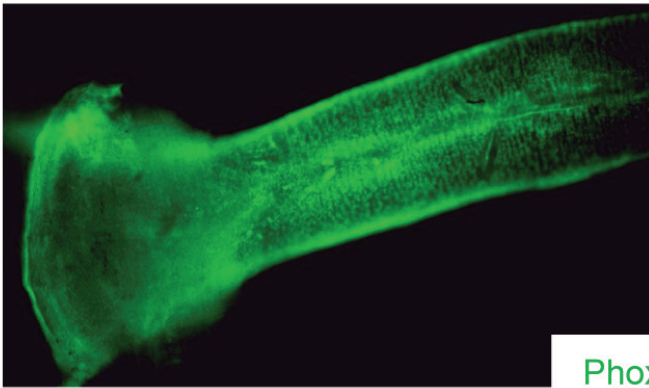
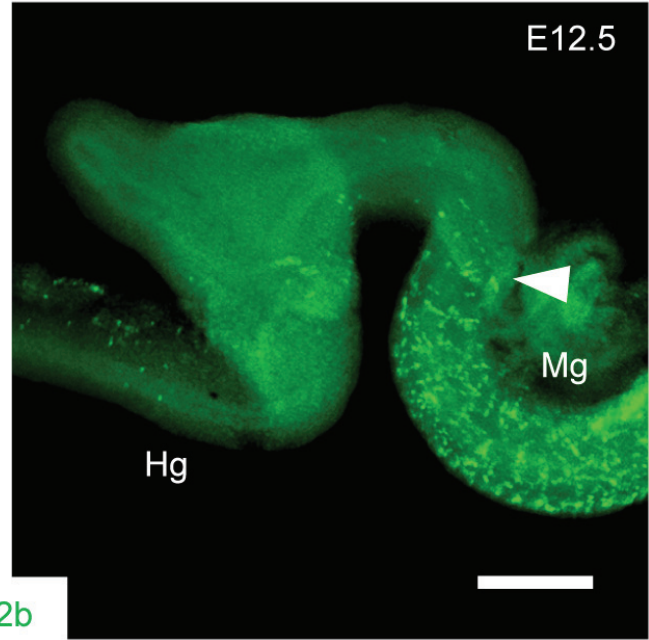
671 gut. White arrowheads indicate the location of wavefront of enteric neurons. **B**,
672 Comparison of location of ENS wavefront between $Ret^{51(C618F)/EGFP}$ and $Ret^{51(C618F)/EGFP}/$
673 $Ednrb^{+/-}$ mice at P0. Reduction of $Ednrb$ gene dosage increased the severity of enteric
674 aganglionosis of $Ret^{51(C618F)/EGFP}$ mice. **C**, Whole-mount GFP staining of the enteric
675 neurons in E12.5 $Ret^{51(C618F)/EGFP}/Ednrb^{+/-}$ gut. White arrowhead indicates location of
676 the wavefront of ENS precursors. **D**, Whole-mount GFP, PGP9.5, Sox10 and pERK
677 pathway stainings of ENS cells of $Ret^{51(C618F)/EGFP}/Ednrb^{+/-}$ embryos at E12.5.
678 Activation of ERK was observed in ENS precursors at the migratory wavefront. **E**,
679 Immunohistochemical detection of GFR α 1 (green) in ENS progenitors (whose nuclei
680 marked in magenta by anti-Phox2b antibody) of wild type, $Gdnf^{+/-}$ and $Ednrb^{+/-}$
681 embryos (E12.5). Ce, cecum; Co, colon; Si, small intestine; Hg, hindgut; Mg, midgut.
682 Scale bars: **A**, 1 mm; **C**, 250 μ m; **D**, 20 μ m.

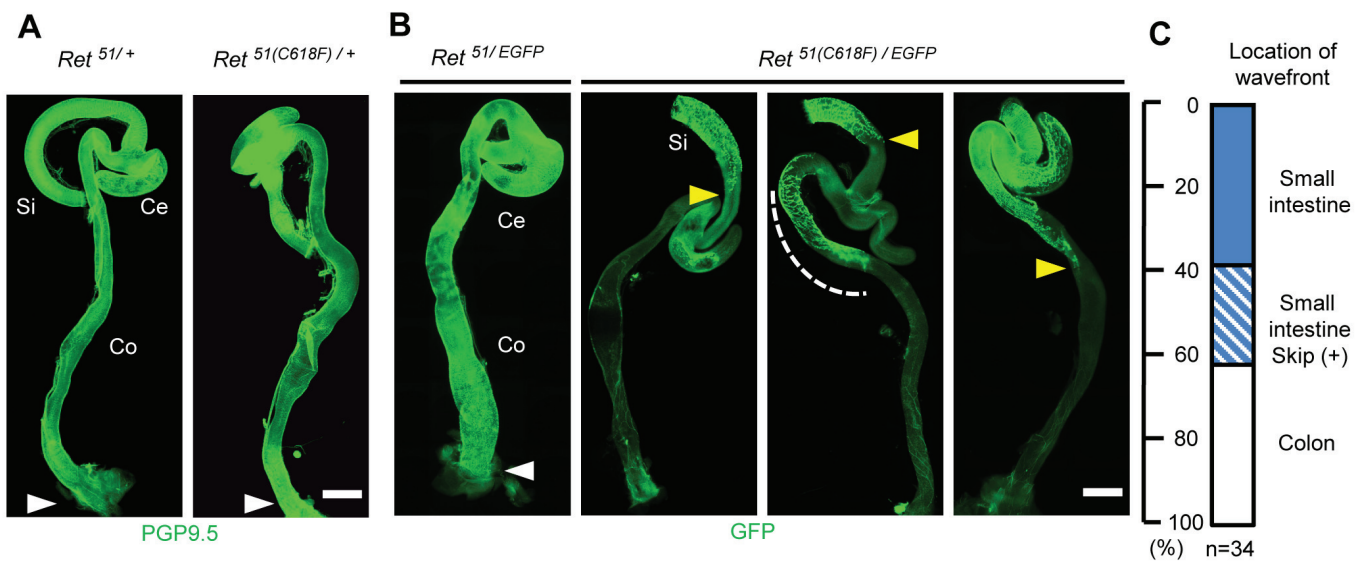


Ret^{51/51}



Ret^{51(C618F)/51(C618F)}

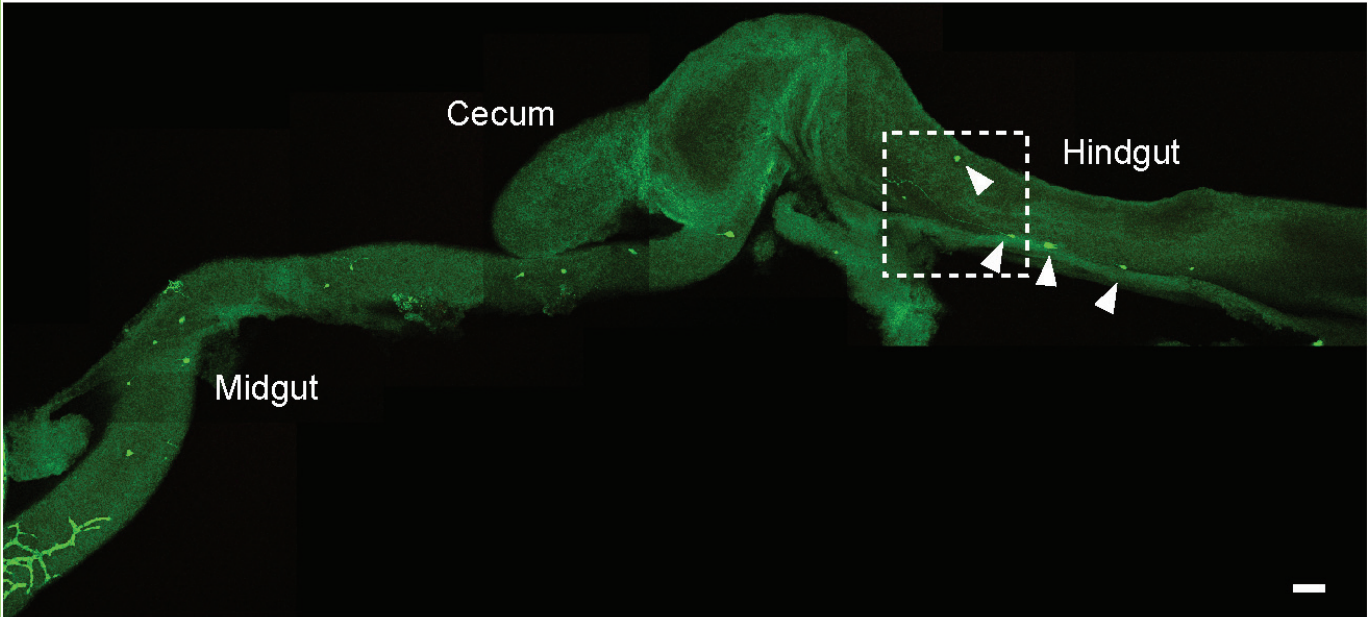




A

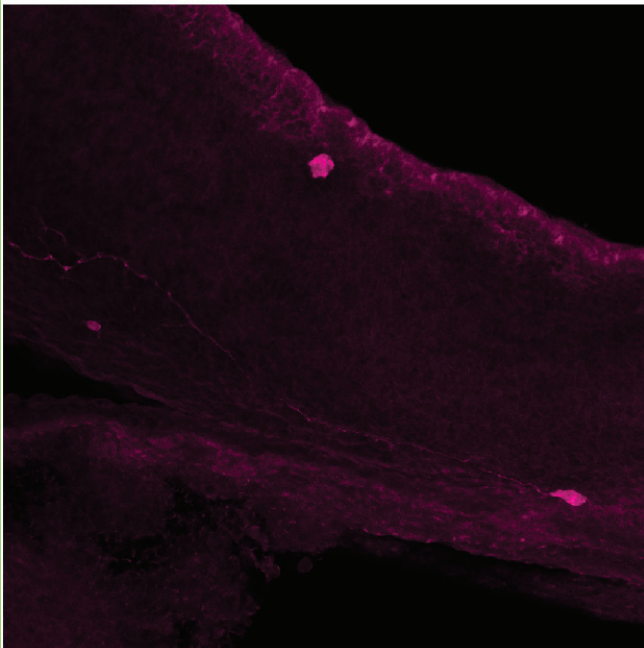
Ret^{51(C618F)/EGFP}

E13.5

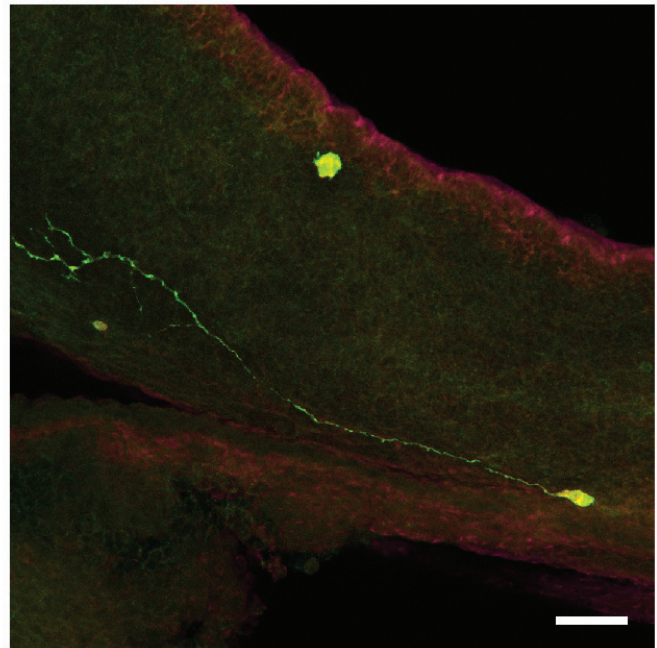


B

EGFP



PGP9.5



EGFP/PGP9.5

